Mechatronics 21 (2011) 993–1002

Contents lists available at ScienceDirect

Mechatronics

journal homepage: www.elsevier.com/locate/mechatronics

Evaluation of the dynamic performance variation of a serial manipulator after eliminating the self-weight influence

Pi-Ying Cheng, Kuei-Jen Cheng *

Department of Mechanical Engineering, National Chiao-Tung University, 1001 University Road, Hsinchu City 300, Taiwan, ROC

ARTICLE INFO

Article history:
Received 9 December 2010
Accepted 27 March 2011
Available online 19 April 2011

Keywords:
Gravity balance
Acceleration radius
Maneuverability ratio

ABSTRACT

Manipulators used in the industrial field usually have a very stiff structure but without an equivalent payload on their end-effectors. This is because the stiff structure is used to prevent excessive deformation which will negatively impact the positioning accuracy of the manipulator, especially when the manipulator is fully extended. However, the stiff structure increases the weight of the manipulator and consumes much of the output of the constituent joint actuators in order to overcome the gravitational force resulting from the heavy structure. To cope with this problem, the concept of gravity balance was proposed decades ago, and there have been several approaches suggested to eliminate the influence of the self-weight of the structure. With the help of gravity balance, the output of the constituent joint actuators can fully be used to drive the manipulator and save considerable energy when the manipulator is in static or low-speed applications.

For decades, many papers have discussed how to make a manipulator in gravity balance or how to design and apply a gravity balance mechanism to satisfy a certain application. However, none of them discuss what the influence on the dynamic performance of a manipulator is after it is equipped with a gravity balance mechanism or how to evaluate that influence. To rectify this insufficiency, this article utilizes acceleration radius to be the index of measuring the dynamic performance before and after a manipulator is equipped with a gravity balance mechanism and proposes a new index, the maneuverability ratio, to provide quantitative information to measure whether the dynamic performance of the manipulator increases or not after the gravity balance mechanism is applied.

1. Introduction

In the industrial field, many kinds of manipulators are designed to do assembly jobs on production lines. One common characteristic of these manipulators is that the weight of their arms is much greater than the payload at their end-effectors. This heavy weight results from the stiff structure which is used to prevent excessive deformation from negatively impacting positioning accuracy, especially when the manipulator is fully extended. The heavy structure increases the demand of the output of the constituent joint actuators which are used to counterbalance the influence of the heavy self-weight. For many applications, manipulators spend most of their work time on static or low-speed jobs and consume considerable amounts of energy to counterbalance their self-weight [1], thus increasing the operational cost.

To cope with this problem, the concept of gravity balance is proposed and successfully counteracts the adverse effects of self-weight. For decades, the gravity balance model and theory have been studied in a large volume of literature [2–22], and many special designs have been developed to successfully satisfy the requirements of different applications [1,23–31]. Meanwhile, the required actuator output which is used to perform a specific task before and after a manipulator has been equipped with a gravity balance mechanism has also been investigated in some studies [32]. However, as far as the author knows, none of the literature discusses what the variation in dynamic performance is before and after a manipulator is equipped with a gravity balance mechanism, and they all focus on how to eliminate the influence of the self-weight or the required actuator output used to perform a specific task after a gravity balance mechanism is applied. Because manipulators are not just designed for or dedicated to static or low-speed applications and certainly not just designed for a specific task, this will lead to insufficient conclusions. How the gravity balance mechanism influences the dynamic performance of a manipulator needs to be considered. To rectify this insufficiency, this article utilizes acceleration radius to evaluate the dynamic performance before and after a manipulator is equipped with a gravity balance mechanism, and this article also proposes a new index, the maneuverability ratio, to provide quantitative informa-

* Corresponding author. Tel.: +886 3 5712121x55154.
E-mail address: waynechen.me94g@nctu.edu.tw (K.-J. Cheng).

0957-4158/$ - see front matter © 2011 Elsevier Ltd. All rights reserved.
doi:10.1016/j.mechatronics.2011.03.006

tion about whether being equipped with the gravity balance mechanism would increase or decrease the dynamic performance of the manipulator.

In order to effectively interpret the concept of gravity balance and explain the proposed methodology of evaluating the variation of the dynamic performance after a manipulator is equipped with a gravity balance mechanism, this article is arranged as follows: Section 2 provides a brief introduction of the fundamentals of gravity balance; Section 3 explains how to derive acceleration radius and conduct maneuverability ratio; Section 4 demonstrates the method proposed in this article with the use of a PUMA 560 robot arm; Section 5 presents the conclusions of this article.

2. Fundamentals of gravity balance

Utilizing the concept of gravity balance to eliminate the self-weight influence of a manipulator usually takes two approaches. One is using counterweights to offset the gravitational force resulting from the self-weight, and the other is utilizing springs and auxiliary links, which include wires and cams, to keep the summation of the gravitational potential energy of the manipulator system and the elastic potential energy of the spring system constant. Although there are still other approaches which are able to keep the manipulator in gravity balance [19,21,25,26], they are rarely used in practice. In the following subsections, the fundamentals of each of the two approaches will be introduced.

2.1. The counterweight approach

Placing the center of mass of a manipulator system at the joint which connects the base and the first link by using counterweights to counterbalance the gravitational force resulting from the weight of each constituent link is possible and feasible. Because the center of mass of the manipulator system is fixed to the base, a static joint, the potential energy of the system will be invariant in any posture. This means no external force needs to be exerted on the manipulator to do any work to change its posture. In this approach, the weight of each counterweight being used is unknown because it depends on the dimensions, configurations, and weights of the constituent links and needs to be calculated. To more clearly demonstrate this approach, a two-link example is shown in Fig. 1, and the weights of the counterweights used in this example are shown in (1) and (2), respectively. For a general case, the weight of each counterweight can be calculated from (3).

$$cm_1 = \frac{m_1 c_1 + (cm_2 + m_2) l_1}{wc_1} \tag{1}$$

$$cm_2 = \frac{m_2 c_2}{wc_2} \tag{2}$$

$$cm_i = \frac{m_i c_i + l_i \cdot \sum_{j=i+1}^{n} (cm_j + m_j)}{wc_i} \tag{3}$$

where n is the link number; cm_i and cm_j are the weights of the counterweights of link i and link j respectively; m_i is the weight of link i; c_i is the distance between the center of mass of link i and joint i; l_i is the length of link i; wc_i is the distance between the center of mass of the counterweight of link i to joint i.

2.2. The spring and auxiliary link approach

Because the elastic potential energy of a spring is proportional to the square of its deformation, and the relation between the posture and the gravitational potential energy of a manipulator system is highly non-linear, there must be some kind of mechanism which is used to transform and match these two energies. Roughly speaking, there are two types of mechanisms which are used to transform and match these two energies. The first one is to utilize cams with specific contours [10,11,24,31], and the other is to use the orthosis or parallelogram mechanisms to accomplish this job [1,2,4,6,7,12–17,20,22,27–29].

In the cam approach, the contours of the cams in use are specialized according to the configuration and the weight arrangement of a manipulator, and the springs will be dragged along with the corresponding contours and compensate for the variation in gravitational potential energy of the manipulator system. A single link system is shown in Fig. 2 and the contour of the cam is depicted in Fig. 3. Assuming the diameter of the wire connecting the spring and the cam is negligible, the contour of the cam for the single link system can be conducted by following (4)–(6) [24].

$$r = \sqrt{\frac{mgl}{2k}} \cdot \left(\sin\frac{\theta}{2} - \cos\frac{\theta}{2} \right) \tag{4}$$

$$r_c = \sqrt{\frac{mgl}{8k}(5 - 3\sin\theta)} \tag{5}$$

$$\delta = \tan^{-1}\left[-\frac{1}{2}(\csc\theta + \tan\theta) \right] \tag{6}$$

where r is the effective radius of the cam; k is the stiffness coefficient of the spring; mg is the effective gravitational force of the self-weight; l is the distance from the joint axis to the location of

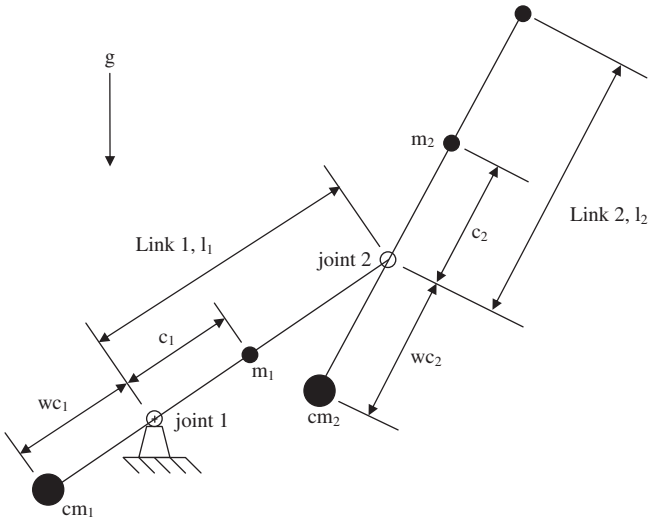

Fig. 1. Two-link example of the counterweight approach.

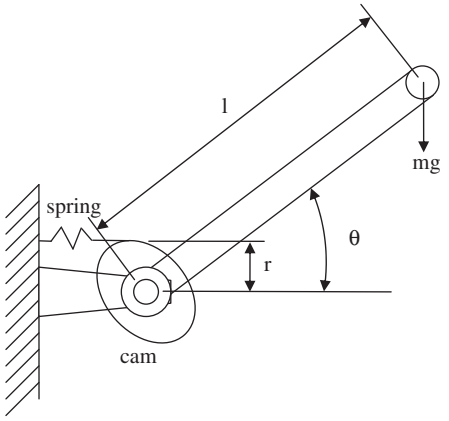

Fig. 2. Single link example of the cam approach.

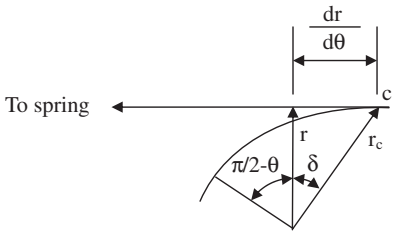

Fig. 3. Contour of the cam.

the effective weight; θ is the angle between the link and the horizontal plane; c is the real leave point of the wire to the cam; r_c is the actual radius following the cam shape; δ is the angle deviation between r and r_c.

The orthosis approach utilizes auxiliary links to create one or several parallelograms among the constituent links of a manipulator to find out or point to the effective center of mass of the manipulator system. It then uses one end of a zero-free-length spring to connect to the joint which corresponds to the center of mass of the manipulator system, and the other end of the spring connects to a certain inertial place. It also uses other zero-free-length springs to connect each parallelogram to a certain place which depends on the link number, configuration, and weight arrangement of the manipulator. Fig. 4 shows a special case of a two-link example which can be used to lift up heavy weight and external force in the gravitational direction with relatively small input force, and the lengths of the auxiliary links ($l_1 - s_1$ and s_2) are expressed in (7) and (8) respectively, and the stiffness coefficients of the springs (k_1 and k_2) can be calculated by (9) and (10) respectively [33].

$$l_1 - s_1 = l_1 - \frac{s_2(m_1 g c_1 + m_2 g l_1 + f l_1)}{m_2 g c_2 + f l_2} \tag{7}$$

$$0 < s_2 < l_2, \quad \text{and} \quad s_2 \quad \text{must satisfy} \quad 0 < s_1 < l_1 \tag{8}$$

$$k_1 = \frac{s_1(m_2 g c_2 + f l_2)}{h s_2 (l_1 - s_1)} \tag{9}$$

$$k_2 = \frac{m_2 g c_2 + f l_2}{h s_2} \tag{10}$$

where f is the external force exerted on the end of link 2 in the gravitational direction; m_1 and m_2 are the masses of link 1 and link 2 respectively; c_1 and c_2 are the distance from the center of mass of

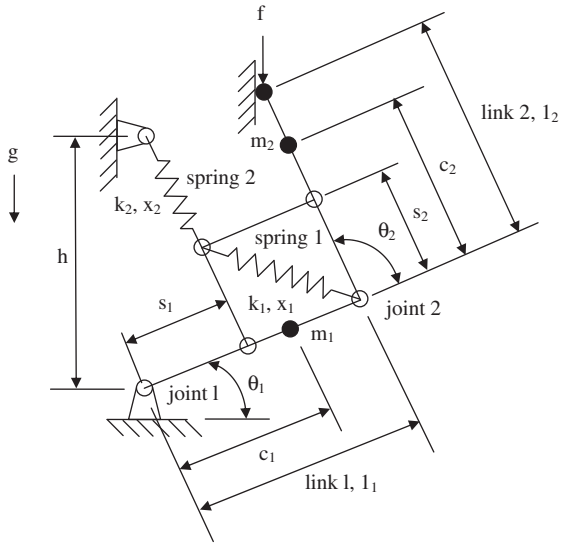

Fig. 4. Two-link example of the orthosis approach.

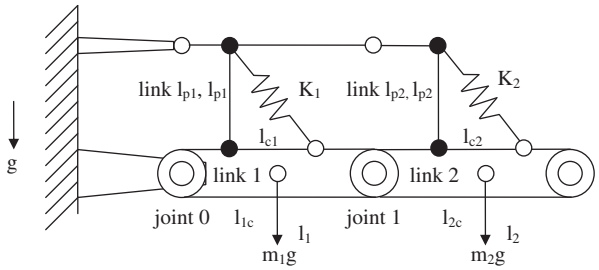

Fig. 5. Two-link example of the parallelogram approach.

link 1 to joint 1 and the distance from the center of mass of link 2 to joint 2 respectively; l_1 and l_2 are the lengths of link 1 and link 2 respectively; h is the vertical distance from one end of spring 2 to the base; θ_1 and θ_2 are the angles from the base to link 1 and the angle from link 1 to link 2 respectively.

As with the orthosis approach, the parallelogram approach also uses auxiliary links to create one or more parallelograms. Differing from the orthosis approach, these parallelograms are not used to identify the center of mass of the manipulator system. Instead they create an environment in which each constituent link of the manipulator can be considered independently. Fig. 5 shows a two-link example of this approach. In this approach, the masses of the auxiliary links and the springs are usually assumed to be negligible. When the masses of the auxiliary links and the springs are negligible as in this example, the stiffness coefficients of the springs can be expressed as (11) and (12), respectively. Also, when the masses of the auxiliary links and the springs are negligible, the general form of calculating the stiffness coefficient of each spring is shown in (13) [22].

$$k_1 = \frac{m_1 g \cdot l_{1c} + m_2 g \cdot l_1}{l_{c1} \cdot l_{p1}} \tag{11}$$

$$k_2 = \frac{m_2 g \cdot l_{2c}}{l_{c2} \cdot l_{p2}} \tag{12}$$

$$k_i = \frac{m_i g \cdot l_{ic} + \sum_{j=i+1}^{n} m_j g \cdot l_i}{l_{pi} \cdot l_{ci}} \tag{13}$$

where k_i is the stiffness coefficient of the spring i; m_i and m_j are the masses of link i and link j respectively; l_{ic} is the distance between joint i - 1 and the center of mass of link i; l_i is the length of link i; l_{pi} is the height which is from the one end of spring i to the connecting joint of link l_{pi} and link i in the gravitational direction; l_{ci} is the distance which is along link i and between the one end of spring i to the connecting joint of link l_{pi} and link i.

Using cams and springs to achieve gravity balance is feasible, but accurately fabricating the cam is usually very difficult because of its highly non-linear surface contour. Using orthosises is feasible and practical, but its application is usually limited to manipulators with few constituent links. This is because the arrangement of the spring highly depends on the configuration and weight arrangement of the manipulator to which it would be applied, and it is not easy to find a feasible one when there are more than two links. For a manipulator with more than two links, the parallelogram approach is usually used to keep the manipulator in gravity balance.

For the majority of manipulators used in the industrial field, there are usually three or more links to assure that they can reach any point in a three-dimensional workspace. Therefore, only the counterweight and auxiliary parallelogram approaches are practical and suitable for manipulators used in the industrial field. As a result, only the counterweight and auxiliary parallelogram approaches will be discussed hereafter.

3. Acceleration radius and maneuverability ratio

This section will introduce how to conduct the acceleration radius and maneuverability ratio of a manipulator. Because most of the manipulators used in the industrial field do not use a redundant configuration to reduce the complexity of control and increase the system reliability, the following will only discuss the acceleration radius and maneuverability ratio of manipulators with non-redundant configurations.

Acceleration radius is a dynamic performance index which is utilized to measure the ability of a manipulator to accelerate its end-effector, and it is defined as the maximum achievable end-effector acceleration in all directions in a certain posture under certain output limits of the constituent joint actuators. A larger acceleration radius implies better dynamic performance. For a given posture, if the value of the acceleration radius is less than the required acceleration, then a manipulator may be unable to perform its assigned dynamic task because of the insufficient acceleration ability in that posture. The following will introduce how to conduct acceleration radius.

The velocity and acceleration equations of the end-effector of a manipulator can be expressed as (14) and (15) respectively [34–36].

$$\dot{x}_n = J_{n\times n}(q)\dot{q}_n \tag{14}$$

$$\ddot{x}_n = \dot{J}_{n\times n}(q)\dot{q}_n + J_{n\times n}(q)\ddot{q}_n \tag{15}$$

where n is the link number; q is the vector of the joint variable; x is the vector of the position variable of the end-effector in the reference frame; $\dot{x}$ is the vector of the end-effector velocity in the reference frame; $\ddot{x}$ is the vector of the end-effector acceleration in the reference frame; $J_{n\times n}$ is the $n \times n$ Jacobian matrix.

The kinetic equation of a manipulator can be expressed as (16).

$$\tau_n = M_{n\times n}(q)\ddot{q} + c_n(q,\dot{q}) + g_n(q) \tag{16}$$

where τ is the vector of the torque of the constituent joint actuators; $M(q)$ is the $n \times n$ inertia matrix of the manipulator; $c(q,\dot{q})$ is the vector of the torque resulting from the centrifugal and Coriolis forces; $g(q)$ is the vector of the torque resulting from the self-weight of the manipulator and the external force.

Rearrange (16), $\ddot{q}$ can be presented as (17).

$$\ddot{q} = M^{-1}(\tau - c - g) \tag{17}$$

Substitute (17) into (15), $\ddot{x}$ can be presented as (18).

$$\begin{aligned}\ddot{x} &= JM^{-1}(\tau - c - g) + \dot{J}\dot{q} \\ &= JM^{-1}\tau + (-JM^{-1}c + \dot{J}\dot{q}) + \left(-JM^{-1}g\right)\end{aligned} \tag{18}$$

where $JM^{-1}\tau$ is the vector of the acceleration which is contributed by the constituent joint actuators; $-JM^{-1}c + \dot{J}\dot{q}$ is the vector of the acceleration caused by the centrifugal and Coriolis forces; $-JM^{-1}g$ is the vector of acceleration resulting from the self-weight of the manipulator and the external force.

Actuators used in the industrial field almost always have the same upper and lower output limits, and they can be expressed as (19).

$$-\tau_i^{\text{limit}} \leqslant \tau_i \leqslant \tau_i^{\text{limit}}, \qquad i = 1 \sim n \tag{19}$$

After normalizing (19), the normalized output vector of the constituent joint actuators, $\hat{\tau}$, can be presented as (20).

$$\hat{\tau} = L^{-1}\tau \tag{20}$$

where L is a diagonal matrix, and the value of each diagonal element is equal to the output limit of the corresponding actuator and can be expressed as (21).

$$L = \begin{bmatrix} \tau_i^{\text{limit}} & 0 & 0 \\ 0 & \ddots & 0 \\ 0 & 0 & \tau_n^{\text{limit}} \end{bmatrix} \tag{21}$$

From (19) and (20), $\hat{\tau}$ has the characteristic shown in (22).

$$\hat{\tau}^T\hat{\tau} \leqslant 1 \tag{22}$$

Substitute (20) into (18), then $\ddot{x}$ and $\ddot{\tau}$ can be presented as (23) and (24) respectively.

$$\ddot{x} = JM^{-1}L\hat{\tau} + \left(-JM^{-1}c + \dot{J}\dot{q}\right) + \left(-JM^{-1}g\right) \tag{23}$$

$$\hat{\tau} = L^{-1}MJ^{-1}\left(\ddot{x} + JM^{-1}c - \dot{J}\dot{q} + JM^{-1}g\right) \tag{24}$$

Substitute (24) into (22), the acceleration ellipsoid can be conducted and expressed as (25).

$$\left(\ddot{x} + JM^{-1}c - \dot{J}\dot{q} + JM^{-1}g\right)^T J^{-T}M^TL^{-T}L^{-1}MJ^{-1}\left(\ddot{x} + JM^{-1}c - \dot{J}\dot{q} + JM^{-1}g\right) \leqslant 1 \tag{25}$$

Substitute $Q = J^{-T}M^TL^{-T}L^{-1}MJ^{-1}$ into (25), a simpler form can be presented in (26).

$$\left(\ddot{x} + JM^{-1}c - \dot{J}\dot{q} + JM^{-1}g\right)^T Q\left(\ddot{x} + JM^{-1}c - \dot{J}\dot{q} + JM^{-1}g\right) \leqslant 1 \tag{26}$$

The value of the acceleration radius is equal to the value of the radius of the smallest inner tangent sphere of the acceleration ellipsoid, and the center of the sphere is coincident with origin of the reference frame.

When a manipulator is equipped with counterweights to achieve gravity balance, extra mass is added to each link which will cause an increase in the moment of inertia, but this mass will eliminate the deleterious effects of the self-weight of each link. The

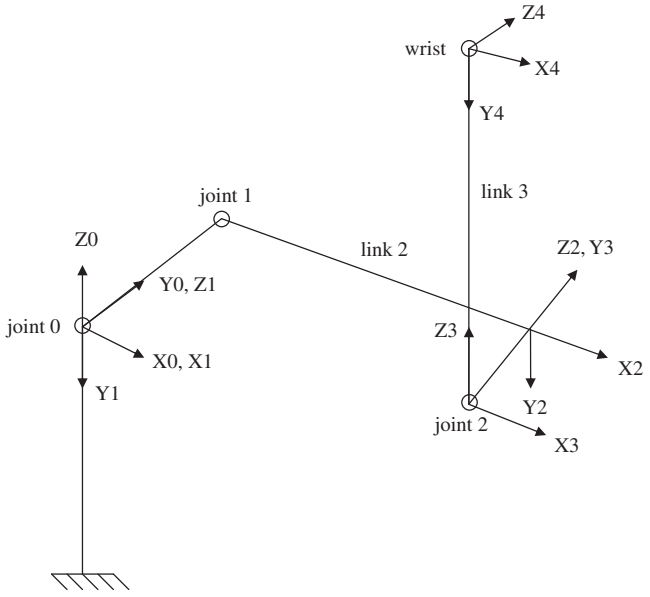

Fig. 6. Zero position with attached frames of the PUMA 560 robot arm.

Table 1
D-H parameters of the first three links of PUMA 560 robot arm.

Frame i	d_i (m)	θ_i (°)	a_i (m)	α_i (°)
1	0	θ_1	0	−90
2	0.2435	θ_2	0.4318	0
3	−0.0934	θ_3	0	90
4	0.4331	θ_4	−0.0203	−90

Table 2
Inertial parameters of the first three links and wrist of PUMA 560 robot arm.

Link i	M (kg)	r_x (m)	r_y (m)	r_z (m)	I_{xx} (kg m^2)	I_{yy} (kg m^2)	I_{zz} (kg m^2)	$I_{xy} = I_{yz} = I_{zx}$ (kg m^2)	Torque Limit (N m)
1	0	0	0	0	0	0	0.35	0	±97.6
2	17.4	0.068	0.006	0.2275	0.13	0.524	0.539	0	±186.4
3	4.8	0	−0.070	−0.0794	0.066	0.0125	0.086	0	±89.4
Wrist	1.25	0	−0.0203	0.4141	0	0	0	0	–

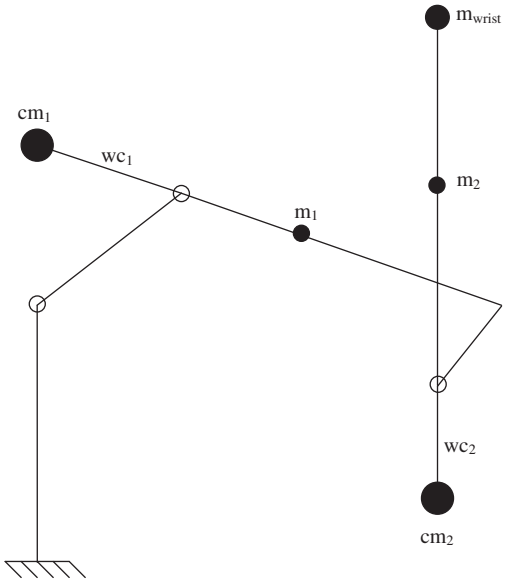

Fig. 7. Skeleton drawing of the PUMA 560 robot arm which is equipped with the counterweights.

Table 3
Parameters of the counterweights.

Counterweight (kg)		Distance (m)	
mc_1	mc_2	wc_1	wc_2
70.62	18.45	0.2	0.05

Table 4
Parameters of the auxiliary parallelograms.

Auxiliary link length (m)				Stiffness coefficient of spring (N/m)	
l_{p1}	l_{c1}	l_{p2}	l_{c2}	k_1	k_1
0.2	0.3	0.2	0.2	1074.34	220.42

Table 5
Angular speed of each joint in the different speed cases.

Joint i	Moderate speed (rad/s)	High speed (rad/s)
0	2	4
1	2	4
2	1	2

acceleration ellipsoid of a manipulator which is equipped with counterweights can be expressed as (27).

$$\left(\ddot{x} + JM_{cw}^{-1}c_{cw} - \dot{J}\dot{q}\right)^T Q_{cw}\left(\ddot{x} + JM_{cw}^{-1}c_{cw} - \dot{J}\dot{q}\right) \leqslant 1 \tag{27}$$

where M_{cw} is the inertia matrix of the manipulator which is equipped with the counterweights; c_{cw} is the vector of the torque caused by the centrifugal and Coriolis forces after the counterweights are applied; $Q_{cw} = J^{-T}M_{cw}^{T}L^{-T}L^{-1}M_{cw}J^{-1}$.

Because the auxiliary links used in the auxiliary parallelogram approach are employed merely to create an environment which can compress or stretch the springs to store the energy, there is no need to have a very stiff structure. Based on this reasoning, the mass of the auxiliary links is very small when it is compared with the mass of the manipulator, and it can be omitted without any significant influence on the dynamic performance. Because the mass of the auxiliary links can be omitted, a manipulator which

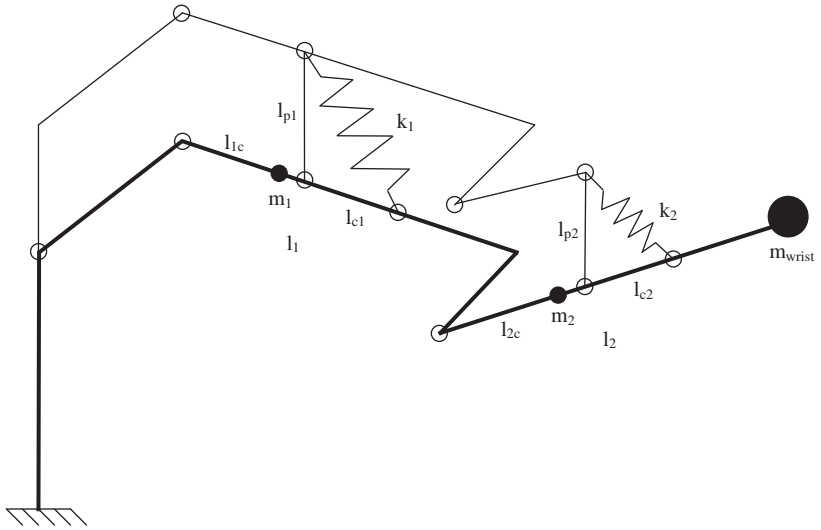

Fig. 8. Skeleton drawing of the PUMA 560 robot arm which is equipped with the auxiliary parallelograms.

is equipped with auxiliary links will have the same inertia matrix and vector of the torque resulting from the centrifugal and Coriolis forces as the unbalanced one. The acceleration ellipsoid of a manipulator which is equipped with auxiliary parallelograms can be expressed as (28).

$$\left(\ddot{x}+JM^{-1}c-j\dot{q}\right)^{T}Q\left(\ddot{x}+JM^{-1}c-j\dot{q}\right)\leqslant 1 \tag{28}$$

Once the acceleration radius of a manipulator is calculated for before and after it is equipped with the gravity balance mechanism, the maneuverability ratio in a certain posture can be defined as (29), and the one in a certain workspace can be expressed as (30). With the help of this index, it is easy to quantitatively evaluate how much the dynamic performance of a manipulator improves or deteriorates after being equipped with a gravity balance mechanism.

$$MR_P=\frac{r_g-r_o}{r_o} \tag{29}$$

where MR_P is the maneuverability ratio in a specific posture; r_g and r_o are the acceleration radiuses after and before being equipped with a gravity balance mechanism respectively.

$$MR_W=\frac{I}{W} \tag{30}$$

where MR_W is the maneuverability ratio in a prescribed workspace; $I=\int_w(MR)dw$ is the integral of the maneuverability ratio over the workspace; $W=\int_w dw$ presents the workspace; MR is the

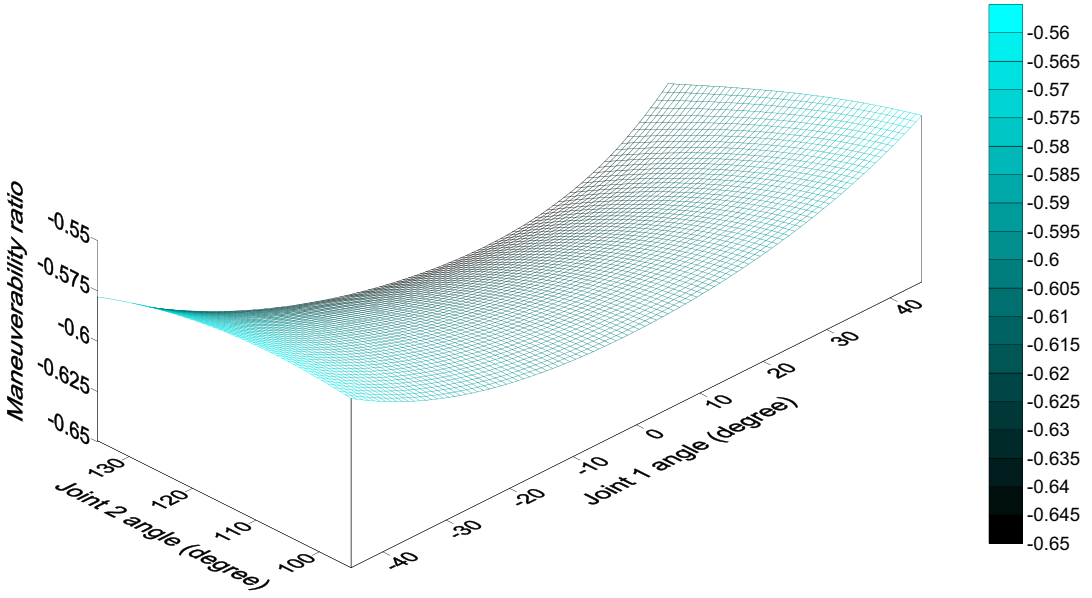

Fig. 9a. Maneuverability ratio distribution in the standing case (a) the counterweight approach.

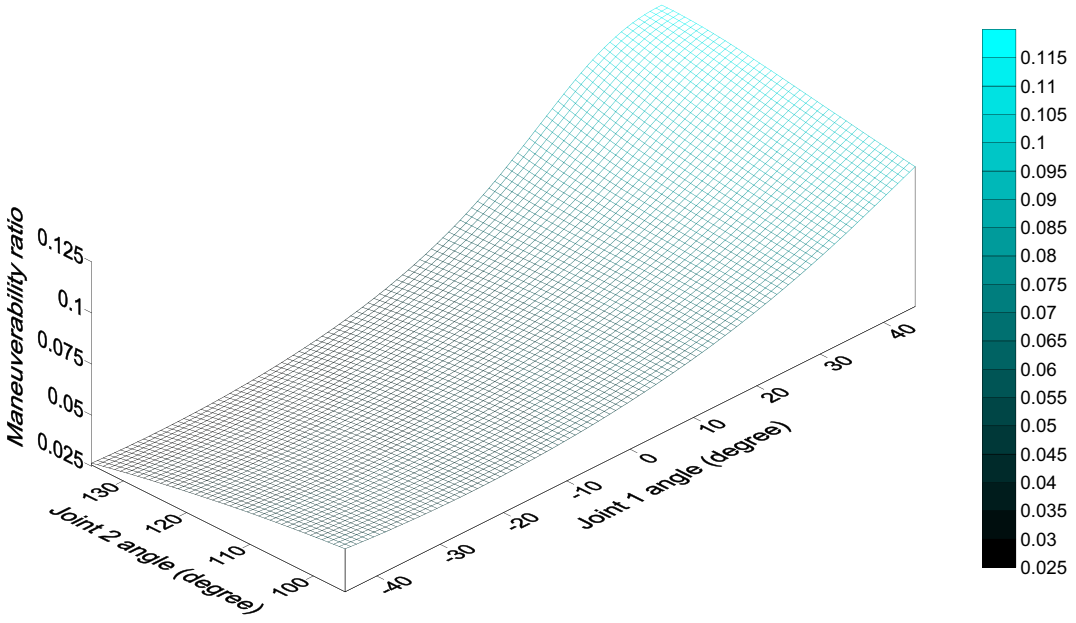

Fig. 9b. Maneuverability ratio distribution in the standing case (b) the auxiliary parallelogram approach.

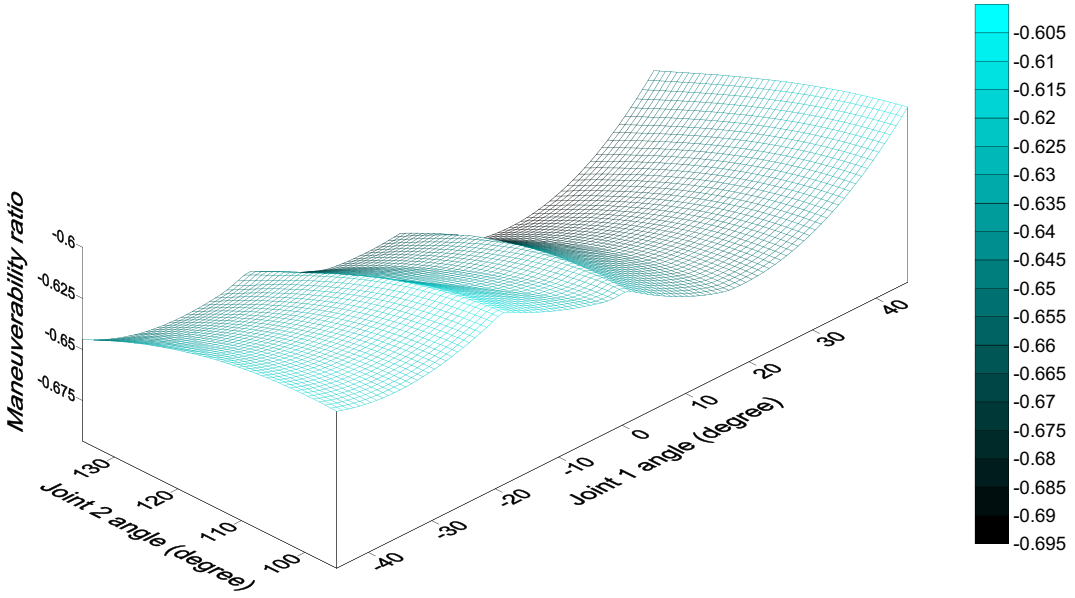

Fig. 10a. Maneuverability ratio distribution in the moderate speed case (a) the counterweight approach.

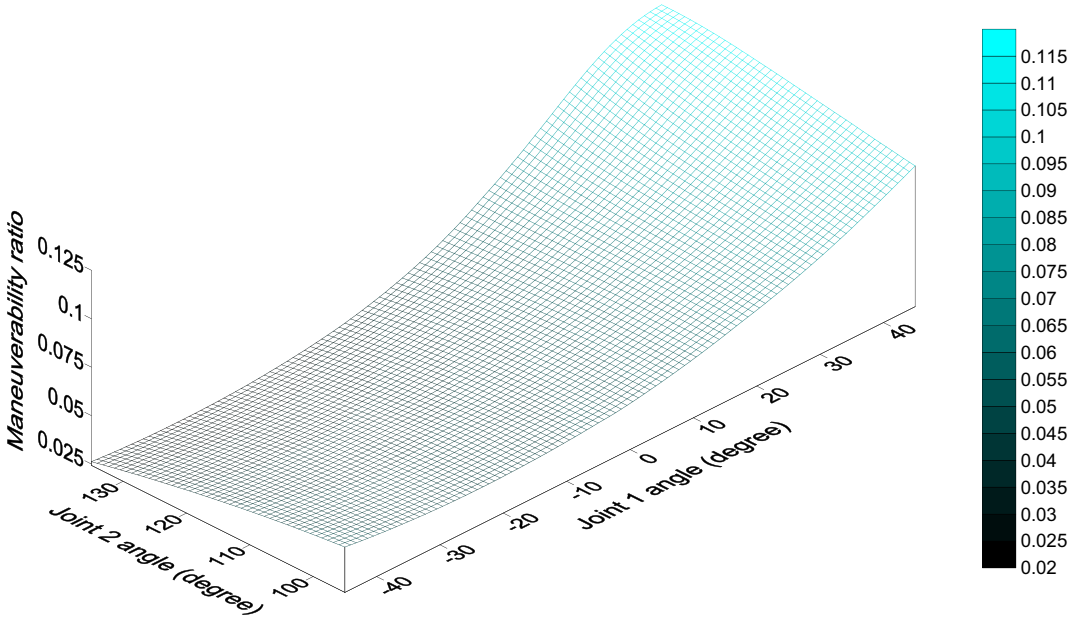

Fig. 10b. Maneuverability ratio distribution in the moderate speed case (b) the auxiliary parallelogram approach.

maneuverability ratio at *dw*; *dw* presents the differential area of the workspace.

If MR_P or MR_W is positive, this means that equipping a manipulator with the gravity balance mechanism will not only eliminate the influence of the self-weight of the manipulator but also improve its dynamic performance. If MR_P or MR_W is negative, this means that the self-weight of the manipulator is eliminated by applying the gravity balance mechanism, but it also sacrifices the dynamic performance of the manipulator.

4. Example

In this section, a PUMA 560 robot arm will be used as an example to demonstrate how to evaluate the dynamic performance variation of a manipulator before and after being equipped with a gravity balance mechanism. Because the last three links of a PUMA 560 robot arm which compose the wrist are not used to achieve or satisfy dynamic performance requirements but are used instead to control the orientation of the end-effector, the last three links will be considered as a mass point on the end of the third link of the PUMA 560 robot arm in the following discussion. Furthermore, the frictional force is omitted, and the workspace in this discussion is limited to the region which covers what is the most used in the pick and place application [36].

The skeleton drawing with the attached frames of a PUMA 560 robot arm in the zero position is shown in Fig. 6. The parameters of Denavit–Hartenberg transformation matrix (D-H parameters) of the PUMA 560 robot arm are shown in Table 1. Table 2 shows the inertial parameters of the constituent links and the output limits of the actuators used in the PUMA 560 robot arm [36–38]. Because the axis of the first joint is parallel to the gravitational

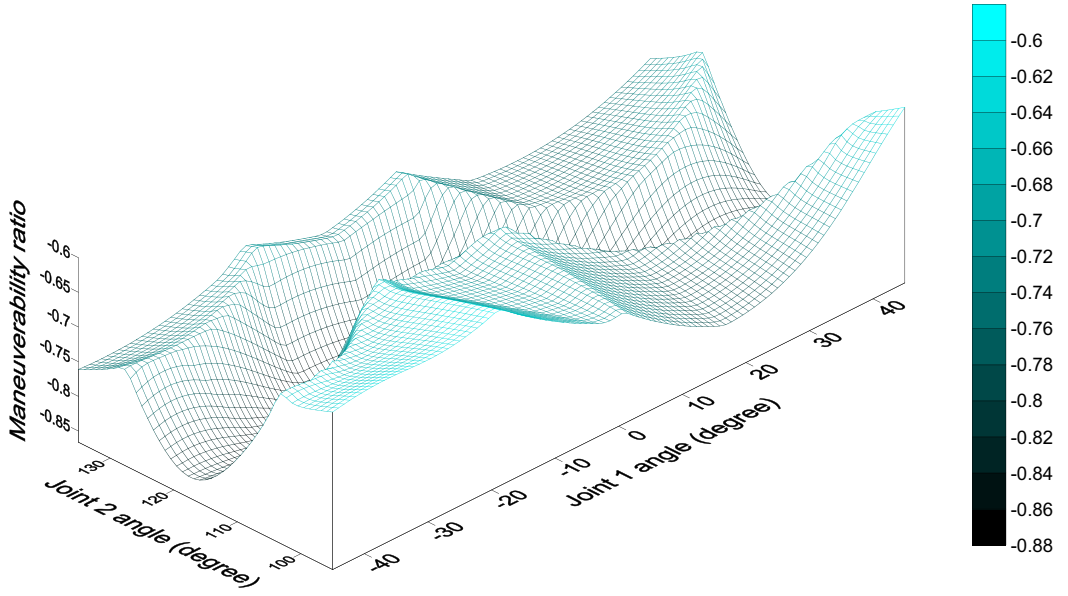

Fig. 11a. Maneuverability ratio distribution in the high speed case (a) the counterweight approach.

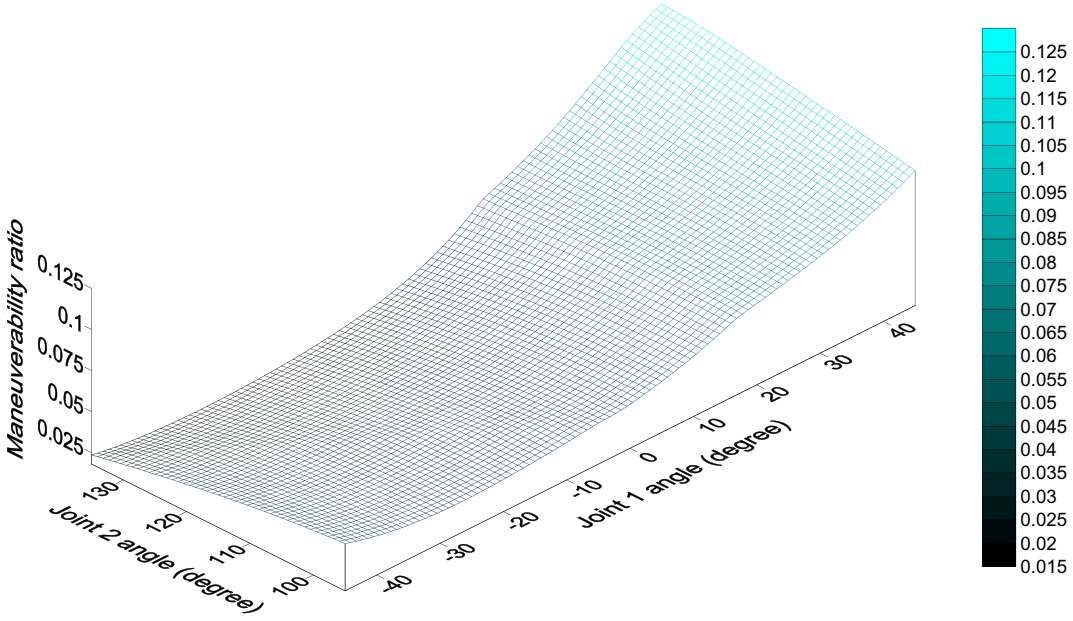

Fig. 11b. Maneuverability ratio distribution in the high speed case (b) the auxiliary parallelogram approach.

direction, the gravitational force does not induce any torque on this joint actuator, and the gravity balance mechanism does not need to be applied to this joint. Fig. 7 shows the skeleton drawing of the PUMA 560 robot arm which is equipped with the counterweights. The corresponding parameters of the counterweights are shown in Table 3. The skeleton drawing of the PUMA 560 robot arm which is equipped with the auxiliary parallelograms is shown in Fig. 8, and the corresponding parameters of the auxiliary parallelograms are shown in Table 4.

There are three cases to consider in the following simulation, and they are respectively: at standing, at moderate speed, and at high speed. Each joint angular speed in the moderate and high speed cases is shown in Table 5. The maneuverability ratio distribution of the robot arm which is equipped with the counterweights in the standing case is shown in Fig. 9a. Fig. 9b shows the maneuverability ratio distribution of the robot arm which is equipped with the auxiliary parallelograms in the standing case. The simulation result of the maneuverability ratio distribution of the robot arm which is equipped with the counterweights at moderate speed is shown in Fig. 10a. Fig. 10b expresses the simulation result of the maneuverability ratio distribution of the robot arm which is equipped with the auxiliary parallelograms at moderate speed. The simulation result of the maneuverability ratio distribution of the robot arm which is equipped with the counterweights at high speed is expressed in Fig. 11a. When the robot arm is equipped with the auxiliary parallelograms at high speed, the simulation result of the maneuverability ratio distribution is shown in Fig. 11b.

In the standing case, the MR_W of the manipulators equipped with the counterweights and the auxiliary parallelograms are −0.6276 and 0.0568 respectively. The MR_W in the moderate speed case is −0.6698 when the manipulator is equipped with the

counterweights, and the MR_W is 0.0567 when the manipulator is equipped with the auxiliary parallelograms. In the high speed case, the MR_W is −0.7783 when the manipulator is equipped with the counterweights, and the MR_W is 0.0544 when the manipulator is equipped with the auxiliary parallelograms. From the simulation results, it is easy to deduce that the dynamic performance of the robot arm which is equipped with the counterweights decreases significantly, and the dynamic performance of the robot arm which is equipped with the auxiliary parallelograms increases moderately. When the angular speed of the constituent joints increases, the dynamic performance of the manipulator which is equipped with the counterweights drops, and the dynamic performance decreases slightly when the manipulator is equipped with the auxiliary parallelograms.

After investigating the simulation results further, some findings were derived and are stated as follows: For the PUMA 560 robot arm, the output torque limit of the actuator at joint 0 is just a little higher than the output limit of the actuator at joint 2 and is just about half of the limit at joint 1. However, joint 0 has the greatest moment of inertia value compared with other two joints in the inertia matrix. This means that, excluding other factors, the output limit of the actuator at joint 0 dominates the dynamic performance of the PUMA 560 robot arm. Because the weight of each link of the PUMA 560 is modest, the influence of self-weight on the dynamic performance is not so significant. When including the influence of self-weight, the output limit of the actuator at joint 0 still dominates the dynamic performance of the PUMA 560 robot arm. This is why the auxiliary parallelogram approach does not promote the dynamic performance as well as expected even though it eliminates the self-weight influence and does not add any extra mass to the robot arm. However, the counterweight approach adds significant mass to the robot arm, especially to link 1, and increases the moment of inertia in joint 0. This is why the dynamic performance is much worse after the robot arm is equipped with the counterweights.

The dynamic performance of the PUMA 560 robot arm which is equipped with the counterweights drops with the increase of the angular speed of the constituent joints because the mass has been increased in each constituent link. When the mass of each link increases, the influence of the centrifugal and Coriolis forces increases and reduces the dynamic performance. This phenomenon can be observed by comparing Fig. 9a with Figs. 10a and 11a; it is obvious that dynamic performance drops significantly with the increase of the angular speed of the constituent joints, especially in certain postures. Because the output limit of the actuator at joint 0 still dominates the dynamic performance in these angular speed ranges, eliminating the influence of the self-weight of each constituent link does not mitigate the load it bears or improve the dynamic performance of the PUMA 560 robot arm. This is the reason why the maneuverability ratio of the PUMA 560 robot arm which is equipped with the auxiliary parallelograms decreases slightly in the simulation results.

5. Conclusions

Gravity balance can help a manipulator consume less energy and reduce the output requirements of the actuators in use when the manipulator is used in static and low-speed conditions. However, manipulators are not designed solely for static and low-speed applications. In many applications, manipulators have to satisfy many dynamic requirements. To rectify this insufficiency, this article utilizes acceleration radius to evaluate the dynamic performance of a manipulator before and after being equipped with a gravity balance mechanism. This article also proposes an index, the maneuverability ratio, to measure the dynamic performance variation before and after a manipulator is equipped with a gravity balance mechanism. An interpretation of the fundamentals of gravity balance is provided in this article, and two of the most practical gravity balance approaches, the counterweight and the auxiliary parallelogram approaches, are chosen to discuss the influence of the gravity balance mechanism on the dynamic performance of a manipulator. In the example, it is easy to deduce that the counterweight approach can eliminate the influence of self-weight, but it also significantly decreases the dynamic performance. The dynamic performance becomes worse with the increase of the joint angular speed when the PUMA 560 robot arm is equipped with the counterweights. When the PUMA 560 robot arm is equipped with the auxiliary parallelograms to counterbalance the self-weight, there is moderate increase in the dynamic performance of the robot arm.

This article provides the methodology and an index to evaluate the influence of the gravity balance mechanism on the dynamic performance of a manipulator. This can not only help the designer of a manipulator to judge whether using a gravity balance mechanism to eliminate the influence of self-weight is beneficial, but it can also help the designer to adjust the setup of the controller which is used to perform the trajectory planning automatically after a gravity balance mechanism is applied. With the help of this article, the designer can also evaluate which kind of gravity balance mechanism will be most beneficial for a given application. From the example, it can be observed that the suitable arrangement of the constituent joint actuators which have different output limits can help a manipulator improve the dynamic performance even after this manipulator is equipped with a gravity balance mechanism, and it also can be observed that the auxiliary parallelogram approach is feasible and better than the counterweight approach in the PUMA 560 robot arm.

References

[1] Bruzzone Luca, Bozzini Giorgio. A statically balanced SCARA-like industrial manipulator with high energetic efficiency. Meccanica 2010. doi:10.1007/s11012-010-9336-6.
[2] Streit DA, Shin E. Equilibrators for planar linkages. ASME J Mech Des 1993;115:604–11.
[3] Yoshikawa Tsuneo, Murakami Hiroki, Hosoda Koh. Modeling and control a three degree of freedom manipulator with two flexible links. Exp Robot II 1993;190:531–45.
[4] Rahman T, Ramanathan R, Seliktar R, Harwin W. A simple technique to passively gravity-balance articulated mechanisms. ASME J Mech Des 1995;117:655–8.
[5] Gosselin Clément M, Wang Jiegao. On the design of gravity-compensated six-degree-of-freedom parallel mechanisms. In: Proceedings of the 1998 IEEE international conference on robotics and automation; 1998. p. 2287–84.
[6] Gokce A, Agrawal SK. Mass center of planar mechanisms using auxiliary parallelograms. ASME J Mech Des 1999;121:166–8.
[7] Roy Jaydeep, Whitcomb Louis L. Comparative structure analysis of 2-DOF semi-direct drive linkages for robot arms. IEEE/ASME Trans Mech 1999;4(1):82–6.
[8] Laliberté Thierry, Gosselin Clément M, Jean Martin. Static balancing of 3-DOF planar parallel mechanisms parallel mechanisms. IEEE/ASME Trans Mech 1999;4(4):363–77.
[9] Simionescu Ion, Ciupitu Liviu. The static balancing of the industrial robot arms. Part I: Discrete balancing. Mech Mach Theory 2000;35:1287–98.
[10] Simionescu Ion, Ciupitu Liviu. The static balancing of the industrial robot arms. Part II: Continuous balancing. Mech Mach Theory 2000;35:1299–311.
[11] Kobayashi Kazuo. Comparison between spring balancer and gravity balancer in inertia force and performance. ASME J Mech Des 2001;123:549–55.
[12] Birglen Lionel, Gosselin Clément M. Kinetostatic analysis of underactuated fingers. IEEE Trans Robot Autom 2004;20(2):211–21.
[13] Agrawal Sunil K, Fattah Abbas. Gravity-balancing of spatial robotic manipulators. Mech Mach Theory 2004;39:1331–44.
[14] Agrawal Abhishek, Agrawal Sunil K. Design of gravity balancing leg orthosis using non-zero free length springs. Mech Mach Theory 2005;40:693–709.
[15] Gosselin Clément M. Adaptive robotic mechanical systems - a design paradigm. ASME Trans Mech Des 2006;128:192–8.
[16] Fattah Abbas, Agrawal Sunil K. Gravity-balancing of classes of industrial robots. In: Proceedings of the 2006 IEEE international conference on robotics and automation; 2006. p. 2872–7.

[17] Hayati Samad A. Assessment of motion of a swing leg and gait rehabilitation with a gravity balancing exoskeleton. IEEE Trans Neural Syst Rehab Eng 2007;15(3):410–20.
[18] Gosselin Clément M. Gravity compensation, static balancing and dynamic balancing of parallel mechanisms. In: Lihui Wang, Jeff Xi, editors. Smart devices and machines for advanced manufacturing. London: Springer; 2008. p. 27–48.
[19] Arakelian V, Ghazaryan S. Improvement of balancing accuracy of robotic systems: application to leg orthosis for rehabilitation devices. Mech Mach Theory 2008;43:565–775.
[20] Lin Po-Yang, Shieh Win-Bin, Chen Dar-Zen. Design of perfectly statically balanced 1-DOF planar linkages with revolute joints only. ASME J Mech Des 2009;131(051004):1–9.
[21] Deepak Sangamesh R, Ananthasuresh GK. Static balancing of spring-loaded planar revolute-joint linkages without auxiliary links. In: Proceedings of the 14th national conference on machines and mechanisms; 2009. p. 37–44.
[22] Lin Po-Yang, Shieh Win-Bin, Chen Dar-Zen. Design of a gravity-balanced general spatial serial-type manipulator. ASME J Mech Des 2010;2(031003):1–7.
[23] Chung Wan-Kyun, Cho Hyung Suck. On the dynamic characteristics of a balanced PUMA-760 robot. IEEE Trans Indus Electron 1988;35(2):222–330.
[24] Ulrich Nathan, Kumar Vijay. Passive mechanical gravity compensation for robot manipulator. In: Proceedings of the 1991 IEEE international conference on robotics and automation; 1991. p. 1536–41.
[25] Homma Keiko, Arai Tatsuo. Design of an upper limb motion assist system with parallel mechanism. In: Proceedings of the 1995 IEEE international conference on robotics and automation; 1995. p. 1302–7.
[26] Uddin Mohammad Jashim, Nasu Yasuo, Mitobe Kazuhisa, Yamada Kou. Application of suspension mechanisms for low powered robot tasks. Int J Indus Robot 2000;27(3):206–16.
[27] MoritaToshio, Kuribara Fumiyoshi, Shiozawa Yuki, Sugano Shigeki. A novel mechanism design for gravity compensation in three dimensional space. In: Proceedings of the 2003 IEEE/ASME international conference on advanced intelligent mechatronics; 2003. p. 163–8.
[28] Fattah Abbas, Agrawal Sunil K, Catlin Glenn, Hamnett John. Design of a passive gravity-balanced assistive device for sit-to-stand tasks. ASME Trans Mech Des 2006;128:1122–9.
[29] Banala Sai K, Agrawal Sunil K, Fattah Abbas, Krishnamoorthy Vijaya, Hsu Wei-Li, Scholz John, et al. Gravity-balancing leg orthosis and its performance evaluation. IEEE Trans Robotics 2006;22(6):1228–39.
[30] Baradat C, Arakelian V, Briot S, Guegan S. Design and prototyping of a new balancing mechanism for spatial parallel manipulators. ASME J Mech Des 2008;130(072305):1–13.
[31] Koser Kenan. A cam mechanism for gravity balancing. Mech Res Commun 2009;36:524–30.
[32] Kolarski Maja, Vukobratovic Miomir, Borovac Branislav. Dynamic analysis of balanced robot mechanisms. Mech Mach Theory 1994;29(3):427–54.
[33] Cheng Pi-Ying, Cheng Kuei-Jen. A gravity balance mechanism used to eliminate the body-weight influence on people with lower-limb disabilities. Technol Disab 2011;23(1):19–28.
[34] Graettinger Timothy J. The acceleration radius – a global performance measure for robotic manipulators. IEEE J Robot Autom 1988;4(1):60–9.
[35] Gosselin C, Angeles J. A global performance index for the kinematic optimization of robotic manipulator. ASME J Mech Des 1991;113:220–6.
[36] Cheng Kuei-Jen, Cheng Pi-Ying. The investigation of the maneuverability deterioration based on acceleration radius theory. Mechatronics 2009;19:1211–20.
[37] Armstrong Brian, Khatib Qussama, Burdick Joe. The explicit dynamic model and inertial parameters of the PUMA 560 arm. In: Proceedings of the 1986 IEEE international conference on robotics and automation; 1986. p. 510–8.
[38] Mozaryn J, Kurek JE. Design of decoupled sliding mode control for the PUMA 560 robot manipulator, In: Proceedings of the 3rd international workshop on robot motion and control RoMoCo 2002, Bukowy Dworek, Poland; 2002. p. 45–50.